A Nanorheological Study of Adsorbed Polymer Layers

P. F. Luckham* and S. Manimaaran

Department of Chemical Engineering and Chemical Technology, Imperial College of Science Technology and Medicine, Prince Consort Road, London SW7 2BY, U.K.

Received August 8, 1996; Revised Manuscript Received May 6, 1997[⊗]

ABSTRACT: In this paper, a means of determining the viscoelastic properties of adsorbed polymer layers under compression is presented. The technique allows rheological properties to be measured on a nanoscopic scale, and revolves around the use of a Surface Force Apparatus (SFA) that has been specially modified for such a purpose. The experiments were carried out by applying an oscillatory motion to one mica surface and monitoring the response of the second confining surface to this motion. The coupling of the motion between the two surfaces is characteristic of the material in the gap and allows the viscoelastic properties of the material to be determined as a function of its confinement. In developing such a technique, the aim was to bridge the gap between the nanoscopic (equilibrium) view obtained from surface force measurements and the macroscopic (dynamic) view obtained from traditional rheological measurements. Results obtained on a PEO/PS system in toluene and a PMMA/PHSA system in a decahydranaphthalene solvent are presented here. The results indicate a significant change in the behavior of the system from being predominantly viscous away from polymer overlap to being predominantly elastic where there is overlap.

Introduction

The stabilization of dispersions by the use of adsorbed polymer layers is of considerable interest both academically and industrially, and the nature of the interactions that take place in such systems have been studied by an ever increasing array of experimental techniques[1,2] and theoretical treatments. The mica-based Surface Force Apparatus (SFA) is one such (experimental) technique[3] and has greatly increased our understanding of the interactions that take place between polymer coated particles.[4] In addition, it has also shed some light on the rheology of polymer-stabilized dispersions.[5] However, to gain further insight into this area requires some knowledge of the dynamics of adsorbed polymer layers. The work presented in this paper describes our attempt and success at modifying the SFA such that it works at a dynamic level.

There are in fact three ways in which the traditional SFA can be adapted to work on a dynamic level. The first of these is one where a lateral motion is applied,[6,7] and this allows systems that are highly confined to be investigated with a view toward understanding their shear and frictional properties. The second is that of a normal oscillatory motion, which can be used at a wide range of separations to measure the viscoelastic properties of the system,[8,9] and the third also revolves around the application of a normal load, but in this case one of the surfaces is held stationary while the other is driven toward it at a constant velocity,[10] allowing the hydrodynamic forces in the system to be measured. It was the second of these techniques that was employed for the purposes of this work.

The modified apparatus designed for the purposes of this work allowed normal dynamic displacements to be applied, at high frequencies, to a confined, adsorbed polymer system. The response of the system was then monitored using a piezoelectric bimorph, with the resulting information processed for the purpose of understanding the mechanisms of the interactions that take place. The apparatus as designed not only drew on the principle features of other designs in this field[8,9] but also incorporated a few new ideas in the form of an electrometer to maintain and amplify the signal from the bimorph and an Inchworm piezoelectric driver for positioning purposes.

The earliest work involving the use of this technique was concerned with the properties of pure solvents[8] and polymer melts[11,12] whereas more recent work by Klein et al.[13,14] has been concerned with the properties of terminally attached polymer layers. The work of Klein et al.,[13,14] though very similar to the work presented here in terms of the types of materials investigated, has revolved around the use of low frequencies ($\omega < 1$ Hz). To this point, no other work has been published detailing the viscoelastic properties of terminally attached polymers, at a nanoscopic scale, at high shear rates—recently, work has been carried out on such systems using an AFM,[15] but the validity of the interpretation of these results is unclear at present.[16] The work of Montfort et al.,[17−19] on a "new" SFA, has thus far been restricted to the study of adsorbed homopolymer layers—to this point their investigations have been the only ones to have considered the properties of confined polymer systems in any detail. No other group has presented "values" for the various moduli at separations where there are polymer interactions, either at low or high shear rates. The possible exploitation of this avenue of investigation by the successful design of a modified SFA was the primary goal of this work. It was also hoped that a study of this nature would facilitate an understanding of macroscopic properties in terms of phenomena observed on a nanoscopic scale and that the theoretical predictions made for such systems could be re-examined in the light of the results obtained.

Interpretation of Raw Data. The Linear Viscoelastic Model

The information retrieved from the apparatus (described in the next section) is converted into meaningful results that describe the viscoelastic properties of the system under investigation, by solving the equation of motion of the lower surface. Such an analysis has already been performed by Montfort and Hadziioannou,[12] and although there are some minor errors in the equation described in their paper, the final expression

[⊗] Abstract published in *Advance ACS Abstracts,* July 15, 1997.

S0024-9297(96)01186-2 CCC: $14.00

shown below takes on a similar form. The expression is derived by summing all the forces that act upon the lower surface which include an inertial contribution, a restoring force, a surface force and a hydrodynamic force. The contribution of the static force can be simplified to a linear function by restricting the dynamic motions to small gap amplitudes.[12] In the case of the hydrodynamic force, the expression is obtained by assuming the existence of a linear viscoelastic fluid, and then adopting a corrected version of the expression derived by Chan and Horn.[10] This leads to a final expression for the storage, G', and loss, G'', moduli shown below:

$$G' = \frac{\bar{D}}{6\pi R^2}\left[(k - m\omega^2)\left(\frac{A_0}{A}\cos\phi - 1\right) - f\right] \quad (1)$$

$$G'' = -\frac{\bar{D}}{6\pi R^2}(k - m\omega^2)\frac{A_0}{A}\sin\phi \quad (2)$$

where $\bar{D}$ is the mean separation, k is the spring constant, R is the radius of curvature of the glass formers, m is the mass of the lever, ω is the frequency at which the experiments were carried out, A is the amplitude of the gap separation, A_o is the amplitude of the imposed motion on the upper surface, ϕ is the phase angle between the motion of the upper surface and that of the gap, and f is the gradient of the force at the mean separation.

In this expression the storage term, G', can be split into two components, one of which relates to the hydrodynamic component, G_H', and the other relating to the equilibrium force contribution, G_c,[18,19] as shown below:

$$G_H' = \frac{\bar{D}}{6\pi R^2}(k - m\omega^2)\left(\frac{A_0}{A}\cos\phi - 1\right) \quad (3)$$

$$G_c = \frac{\bar{D}f}{6\pi R^2} \quad (4)$$

The latter term arises from the compression of the polymer chains and can be calculated from the force distance profiles. The two hydrodynamic terms, however, can only be retrieved from dynamic experiments.

Apparatus

As in the traditional surface force apparatus (SFA),[3] the apparatus designed here made use of two mica-bearing surfaces mounted in crossed cylinder geometry with the mica partially silvered on the reverse side so as to allow the use of light interferometry. However, the apparatus employed here was modified in a number of significant ways, when compared to other well-documented designs, in an attempt to enhance its ease of usage, performance, and to reduce the machine time cost of the instrument. The elaborate driving mechanism involving the use of a number of motors and motion reducing springs was replaced, here, by a piezoelectric micropositioner (Inchworm). This is a commercially available device marketed by Burleigh Instruments Ltd., St Albans, U.K., and consists of three piezoelectric ceramics: a cylindrical one, which expands or contracts along its major axis when a potential difference is placed across it, and two clamping piezos, one at each end of the piezo cylinder. Motion is achieved by alternately expanding and contracting the cylindrical piezo while clamping and declamping the terminal piezos.[20] The cylindrical piezo can thus be driven in either direction with a total travel of around 2.5 cm, and with it an affixed push rod. The motion takes place in ~0.5 nm increments, and the rate of travel can be varied between <1 nm/s and 10 mm/s.

The micropositioner was mounted on the outside of a stainless steel vessel, and the push rod (also attached to the lower surface) passes through an aperture in the lid of the vessel. The aperture is then sealed with a flexible poly(tetrafluoroethylene) diaphragm in order to prevent contamination of the vessel and to prevent solvent evaporation. The use of the Inchworm motor does not necessarily improve the SFA, but it does make the equipment significantly easier to machine and maintain.

The successful measurement of viscoelastic properties required further modifications to the apparatus. The equipment used for this purpose was housed inside the vessel and is shown schematically in Figure 1. The upper glass former was attached to a piezoelectric cylinder of dimensions 12.7 mm (outer diameter) × 1.6 mm (width) × 12.7 mm (length) supplied by Morgan Matroc Ltd., Hampshire, U.K., as in the traditional apparatus, whereas the lower surface was mounted onto a stiffened piezoelectric ceramic bimorph—the bimorph of dimensions 30 mm (length) × 12.25 mm (width) × 0.5 mm (thickness) was also supplied by Morgan Matroc Ltd., Hampshire, U.K. When a potential difference is placed across the inner and outer surfaces of the piezo cylinder, it expands along its major axis. The upper surface can thus be oscillated sinusoidally by placing an a.c. voltage across the piezocylinder. The oscillation applied to the upper surface is transmitted via the material in the intersurface gap, to the lower surface. The transmitted motion as picked up by the lower surface results in a potential difference being developed across the bimorph to which it is attached.

Monitoring and storing the signals for the relative amplitudes and phase angles between the motions for the two surfaces allows the shear moduli of the materials being investigated to be determined. In reality, the signal obtained from the bimorph is very weak (typically a few microvolts under current experimental conditions) and has a very short half-life. As such signals are incredibly difficult to monitor, the output signal from the bimorph was fed to an electrometer prior to being analyzed. The electrometer used was built specifically for the purposes of this work by the Electronics section of the Department of Chemical Engineering, and serves a dual purpose in that it both maintains and amplifies the signals that are fed into it. The presence of a high impedance amplifier negates the effects of drift and decay in the signal from the bimorph.[21] The electrometer does introduce a slight phase angle to the signals being monitored, but these are removed by the use of calibration runs.

The signal emerging from the electrometer was then analyzed using a Solartron 1250 Frequency Response Analyser (FRA) supplied by Schlumberger Electronics Ltd, Hampshire, England. The analyzer was capable of measurements of equal sensitivity to a lock-in amplifier but has the ability to filter out the d.c. bias emanating from the electrometer without inconvenience. The analyzer was also used to provide the input signal to the upper surface. There was however, one limitation which could not be overcome with this apparatus, namely that of working at frequencies <10 Hz. This

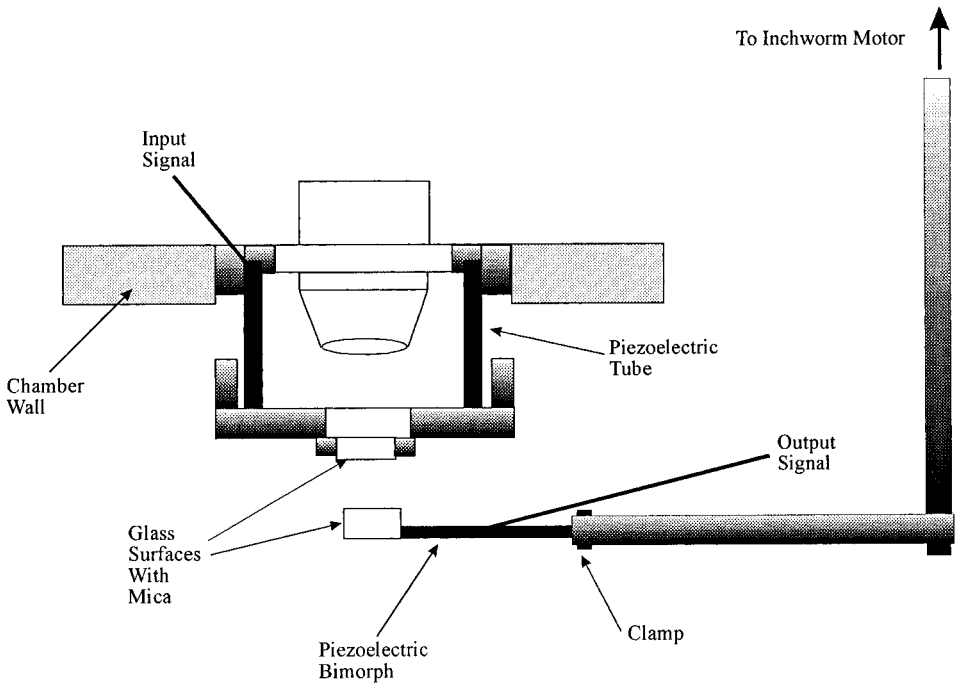

Figure 1. Schematic representation of the dynamic surface force apparatus (DSFA).

arises due to a drop in performance of electronic equipment, in general, at lower frequencies, which could not be accommodated within the required sensitivity of measurements. An oscilloscope was also used to monitor the signal as it was found to be useful for a number of reasons—it confirmed the output signal to be sinusoidal and provided visual proof of the signals being monitored.

In carrying out the experiments it was imperative to minimize errors incurred by minimizing the reliance on the most sensitive parameters of the measurements. In dynamic experiments, the most sensitive measurement relates to the amplitude ratio (A_o/A), and by referring to eqs 1 and 2, it is clear that the only two parameters that could be varied in order to achieve maximum resolution were (i) the spring constant, k, although this had to satisfy the requirement that the resonance frequency of the spring was considerably higher than that of the applied signal, so that inertial effects could be ignored i.e. $\omega_{res} \gg \omega$, and (ii) the applied amplitude, A_o, which was constrained by the limit that the resulting gap amplitude, A, had to be much smaller than the gap separation; i.e. $A \ll D$.

The first of these parameters was in fact the most useful, and the lower frequency limit was of no concern, as a high spring constant is the favored option, which satisfies the requirement of reducing the sensitivity of the measurements to the amplitude ratio, A_o/A. Prior to stiffening, the bimorph exhibited resonance at a frequency of ~70 Hz. Attachment to a brass plate increased the stiffness, resulting in resonance at frequencies >200 Hz. Carrying out experiments at frequencies an order of magnitude below resonance ensured the validity of the results, as mechanical effects emanating from the apparatus would have been minimal. However, it was not possible to increase the value of the spring constant indefinitely and, in this case, past a value much greater than 10 000 N/m, due to the following problems: (i) there was a loss of signal, (ii) the clamps used were not capable of holding a much stiffer spring—there was insufficient room inside the apparatus to make the clamps out of thicker/stiffer material, and (iii) it was very difficult to stabilize the electrometer at amplifications greater than 100×.

Under these circumstances it was found that there was a rather minimal difference between the calibrated signal, and that of the response, A_L, which was measured at high compression, where there are strong equilibrium interactions between the adsorbed layers. The significance of this being that the gap amplitude, $A \rightarrow 0$ under such conditions. The most obvious impact of a very low value for A is that the ratio $A_0/A \rightarrow \infty$, which when added to the fact that A and ϕ_L approach values that are of similar magnitude to the errors involved in the measurements meant that experimental errors could not be ignored in determining the moduli when these values are substituted into eqs 1−3. This does not detract from the worth of the results though, as they are of the right magnitude but not necessarily of the correct value. This accounts for the observed variation of the moduli with separation, at high compression (see Results section). This does not imply that there would be no variation with separation but that the rather random nature of the variation is indicative of the aforementioned errors.

Experimental Procedure

The experiments were conducted by first bringing the two mica bearing surfaces into hard contact and carrying out a calibration run. This was achieved by applying a number of signals to the upper surface via the frequency response analyzer (FRA) and monitoring the response of the lower surface, once again using the FRA. The amplitude of the response signal in hard contact compared to that which is observed with material between the surfaces gives the ratio between the motion that is applied and that which is characteristic of the material in the gap. The calibration runs also provide one other vital source of information, and this is with regard to the "health" of the apparatus. This condition was determined by the fact that the response signal was both consistent with respect to a predetermined optimal standard and similar to those of previous experimental runs. If a significant change in the signal was observed, it was almost always due to a problem with the clamping of the lower surface. This was in fact a major problem that had to be

overcome with an apparatus of this type. Confirmation of the condition of the apparatus was achieved by carrying out numerous calibration runs during the course of a day before the polymer solution being investigated was injected between the surfaces. It needs to be emphasized here that, if the calibration readings taken, typically over a 3−4 h period, are found to vary significantly, the experiment had to be abandoned and the apparatus reassembled.

Once the apparatus was found to be in good working order, the mica surfaces were then separated by ~ 2 mm, and the polymer solution was injected between the surfaces. In the case of a volatile solvent a small amount of solution was also injected onto a piece of filter paper that was placed inside the apparatus, in order to reduce the rate of solvent evaporation.

The polymer solution used, was prepared in a class 1000 clean room to the required concentration, and the syringe was filled in a laminar flow hood located in the clean room. All glassware involved in this process was cleaned thoroughly in ethanol and dried in a laminar flow hood prior to use. The polymer solution was then injected in between the surfaces and left to equilibrate in the apparatus. The surfaces were then gradually brought together until no further motion was possible. This position signifies the maximum compression of the adsorbed polymer layers, and the system was then allowed to settle at this position.

A known, precalibrated signal was then applied to the upper surface of the apparatus using the FRA and the motion of the lower surface monitored. The positional readings and the corresponding position of the Inchworm were recorded on a computer. The response signal from the lower surface at a given separation was then recorded using the FRA. The Inchworm was then used to separate the surfaces gradually, with readings taken at a number of consecutive positions. This procedure was continued until the signal from the bimorph was very weak. The experiment can then be repeated with a new signal after the surfaces are brought back into the position of maximum compression and allowed to settle. The effective shear rate applied during these dynamic experiments varies according to the gap separation, and the amplitude and frequency of the applied motion; however, the shear rates vary between 0.1 and 100 s^{-1}.

The force−distance profiles obtained during dynamic experiments were not as sensitive as ones reported by other workers, due to the fact that much stiffer springs (at least 100×) need to be used to satisfy the requirements of a dynamic experiment. Accurate force−distance profiles require the use of weak springs (k < 100 N/m) as such levers are significantly more sensitive to small forces and motions. Consequently, the profiles used to determine the interparticle forces which in turn were used to determine the static contribution, G_c, to the storage modulus, G'', were achieved when the normal (weak) spring replaced the bimorph. However, the polymer solutions used for these nondynamic experiments were always the same as the ones used for the corresponding dynamic experiments for the sake of compatibility.

The basic surface force experiments require the same procedures to be followed as the dynamic ones except that there was no longer a need to calibrate the apparatus for a number of hours.

Materials. The experiments conducted during the course of this study were restricted to copolymers (in good solvents) as they are better suited to satisfy the dual requirements of steric stabilization of suspensions than are homopolymers. The two polymers on which studies have been carried out were chosen such that they offered some contrast in their properties. The first polymer chosen was a low molecular weight polymer consisting of poly(12-hydroxystearic acid) [PHSA] side chains grafted onto a poly(methyl methacrylate) [PMMA] backbone (which acted as the anchor) with decahydranaphthalene as their solvent (see Table 1). This relatively small polymer was chosen for initial studies as surface force work[5] had already been conducted on this system and as polymers of this type can also be incorporated into polymer latex particles allowing osmotic pressure and rheology measurements to be carried out on them.[5,22,23] The extent and variety of work carried out on this system made it an ideal choice for meaningful comparisons to be made between bulk and nanorheological properties.

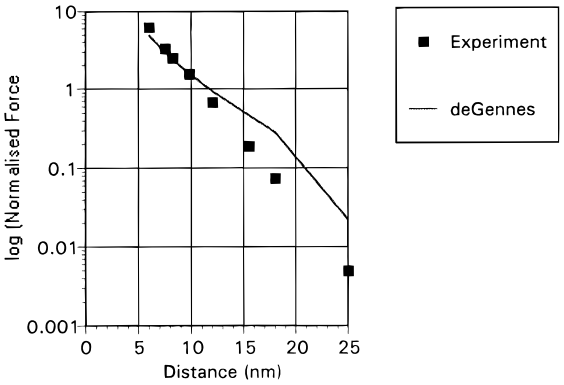

Figure 2. Semilog plot comparison of experimental force data, for PMMA/PHSA in decahydranaphthalene, and de Gennes theory, eq 5, taking a value for s of 1.0 nm and L of 14.0 nm.

Table 1. Material Properties of the Two Polymer Systems Studied

	system I	system II
tot. mol wt (M_w)	20 000	250 300
buoy group	PHSA	PS
buoy group mol wt	2000	229 000
M_w/M_n	unknown	1.14
anchor group	PMMA	PEO
medium	decahydranaphthalene	toluene

The second, a high molecular weight AB block copolymer, consisted of poly(ethylene oxide) [PEO] and poly(styrene) [PS] and used toluene as the solvent. In this system, the PEO acted as the anchoring group, while the PS was the "buoy" polymer extending out into the solvent. The contrast offered by this system was 2-fold—being of high molecular weight (see Table 1), it extended out further into solution than the first system, thereby offering a larger region of polymer interaction for investigation. In addition, it also allowed investigations to be carried out on a volatile solvent such as toluene, which could be used to demonstrate the versatility of the apparatus designed—the "new" SFA used by Montfort et al. is restricted to nonvolatile solvents.[17] It should be noted however, that in the case of volatile solvents, solution injection and experimental measurements had to be carried out on the same day here, and consequently, the data produced may not correspond to equilibrium coverage.

Results

(a) Force Distance Profiles. The force distance profiles for the two systems investigated can be seen in Figures 2 and 3. In the case of experiments involving the PHSA system, measurements were carried out on a 2% by weight solution of the polymer, and for experiments involving the PEO/PS system, a system concentration of 10 μg/mL was used. All results were obtained during decompression cycles, show a purely repulsive variation of force with separation, and are in excellent agreement with those reported by other workers in the field.[5,24] There was no noticeable hysteresis in any of the data obtained in line with observations of others for terminally attached polymers and for copolymers; the decompressions only are shown because in the dynamic experiments described below the data were obtained on decompression cycles. The figures clearly demonstrate the difference in interaction range between the two systems—the adsorbed layer thickness in the case of the PHSA system can be seen to be ~13 nm cf. 110 nm in the case of the PEO/PS system. The significance of this observation will be dealt with in the next section. The figures also show the favorable comparison obtained

Table 2. Response of PMMA/PHSA System at 30 Hz[a]

D (nm)	amplitude, A_L (mV)	phase angle, ϕ_L (deg)	G_c (Pa)	av G_H' (Pa)	av G'' (Pa)	complex viscosity, η^* (mPa s)
6.1	44.19 ± 0.02	1.27 ± 0.00	0.03	0.80	0.74	5.78
8.8	44.15 ± 0.03	1.30 ± 0.02	0.02	1.01	0.88	7.10
10	43.93 ± 0.01	1.62 ± 0.02	0.015	0.51	0.51	3.83
22.3	42.15 ± 0.05	2.48 ± 0.07	∼0	0.34	0.17	0.77
33*	41.96 ± 0.04	3.22 ± 0.05	0	**0.09** *(0.2)*	**0.07** *(0.16)*	**0.61** *(1.36)*
107*	41.32 ± 0.06	10.33 ± 0.22	0	**0.15** *(0.17)*	**0.43** *(0.48)*	**2.42** *(2.70)*
260.1*	36.30 ± 0.00	26.91 ± 0.01	0	**0.08** *(0.08)*	**0.43** *(0.45)*	**2.32** *(2.42)*

[a] Calibration signal (average): 44.37 mV; 1.05°. Error: ± 0.07 mV; ± 0.10°. Solvent viscosity at 20 °C: 2.35 mPa s.

Table 3. Response of PEO/PS System at 25 Hz[a]

D (nm)	amplitude, A_L (mV)	phase angle, ϕ_L (deg)	G_c (Pa)	av G_H' (Pa)	av G'' (Pa)	complex viscosity, η^* (mPa s)
45	25.74 ± 0.02	1.73 ± 0.03	0.15	4.57	2.56	33.35
47	25.65 ± 0.01	1.80 ± 0.02	0.12	3.77	1.88	26.82
51	25.81 ± 0.01	1.63 ± 0.02	0.10	7.46	4.00	53.89
53.5	25.64 ± 0.01	1.75 ± 0.02	0.06	4.43	1.90	30.69
63	25.64 ± 0.01	1.85 ± 0.04	0.03	4.87	2.52	34.91
79	25.39 ± 0.02	1.94 ± 0.03	<0.01	3.91	1.54	26.75
106.4	25.10 ± 0.01	2.14 ± 0.01	∼0	3.59	1.32	24.35
120	24.01 ± 0.03	2.49 ± 0.07	∼0	1.88	0.47	12.34
138	22.54 ± 0.04	3.95 ± 0.06	∼0	1.12	0.38	7.53
162	22.41 ± 0.06	5.90 ± 0.11	∼0	1.06	0.62	7.82
209.6	19.49 ± 0.08	15.48 ± 0.04	∼0	0.44	0.49	4.19
276	13.46 ± 0.12	53.86 ± 0.20	0	**0.001** *(0.015)*	**0.06** *(0.14)*	**0.38** *(0.90)*

[a] Calibration signal (average): 26 mV; 1.41°. Error: ± 0.05 mV; ± 0.02°. Solvent viscosity at 20 °C: 0.59 mPa s.

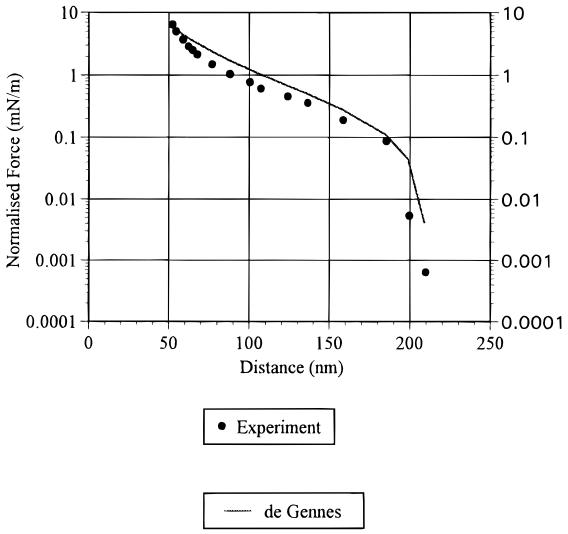

Figure 3. Semilog plot of PEO/PS force data and comparison with de Gennes theory, eq 5, taking a value for s of 5 nm and L of 225 nm.

when the measured force profiles were compared to the theoretical fit predicted by de Gennes.[25]

In the scaling approach for the interaction between polymer brushes, the interaction force between brushes is thought to be made up of two components: (i) the osmotic pressure contribution, and (ii) the elastic restoring force.

As the two polymer-bearing surfaces begin to interact, the osmotic pressure increases as it favors maximum expansion of the chains into solution, whereas the elastic restoring force decreases as it favors a compressed (i.e. less stretched out) structure. At equilibrium, the result of these two contributions must be equal to the overall force, resulting in an expression of the form

$$F = \frac{k_B T}{s^3}\left[\left(\frac{1}{u}\right)^{9/4} - (u)^{3/4}\right] \qquad (5)$$

where s is the average distance between attachment points and $u = d/L$ where d, is the thickness of the compressed layer and L is the thickness of the uncompressed layer. The first term in the above expression accounts for the osmotic pressure and the latter term accounts for the restoring force with the minus sign indicative of their opposing nature. In Figures 2 and 3, s has values of 1 and 5 nm, respectively, and L has values of 14.0 and 112.5 nm, respectively.

(b) Dynamic Experiments. A summary of the results obtained using both the PHSA and PEO/PS systems can be referred to in Tables 2 and 3. The results refer to a typical set of readings taken at a given frequency for each of the two systems. As the frequency range investigated was very narrow (10−30 Hz), little variation was detected in the measurements of the moduli as a function of frequency, and thus a single frequency was thought to suffice for each system.

The results presented correspond to measurements of amplitude to an accuracy of ∼1 nm and phase of ∼0.2°. The results relating to the PHSA system correspond to measurements involving a lower surface exhibiting resonance at 225 Hz and a spring constant of 7630 N/m, whereas those involving the PEO/PS system correspond to resonance at 234 Hz and a spring constant of 10 350 N/m. In the tables, the readings for gap separation accompanied by an asterisk refer to measurements at positions where there were no polymer interactions, with the corresponding values in italics relating to a gap separation corrected for after subtracting the adsorbed polymer layer thickness. Such a procedure is necessary away from polymer overlap, as the model used for the interpretation of data works by presuming the existence of a single uniform material between the two confining surfaces.[12] This is clearly not the case away from overlap, and consequently the model is corrected by assuming the polymer layers take on the form of an extended surface, with minimal participation in the overall flow. This assumption is reasonably well founded and has been supported by theory.[26] However, the greatest concern with such an

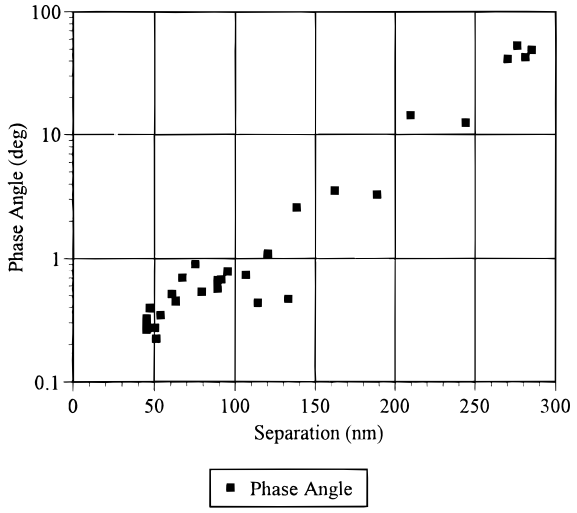

Figure 4. Semilog plot of the variation of phase angle with separation for the PEO/PS system at 30 Hz.

assumption relates to the extent of polymer nonparticipation, and this point will be dealt with in more detail in the next section.

The results obtained for both systems show a number of interesting features that are summarized below. These points will be discussed in more detail in the next section.

(i) At high compression (D < 25 nm for the PHSA system and D < 210 nm for the PEO/PS system), it is noticeable that the hydrodynamic storage modulus, G_H', and the loss modulus, G'', whose origins are purely hydrodynamic, are significantly larger than the frequency independent storage component, G_c, which arises from the equilibrium interactions.

(ii) In addition, at high compression, the storage modulus, G_H', is of the same order of magnitude as but slightly larger than the loss modulus, G''.

(iii) At large separations where there are no steric interactions (D > 33 nm for the PHSA system and D > 210 nm for the PEO/PS system), the loss modulus, G'', dominates, in that it is significantly larger than, the storage contribution, G_H'. In addition, at these separations the results can be reinterpreted to a viscosity reading by making use of the identities quoted below:

$$\eta' = G''/\omega$$

$$\eta'' = G'/\omega$$

which can then be substituted into

$$\eta^* = \eta' - i\eta'' \tag{6}$$

In doing so it was found that, especially in the case of the PHSA system, the values returned for the complex viscosity were very similar to those of the pure solvent.

(iv) The results as shown in Figure 4 displays the transition of the PEO/PS system from a viscoelastic solid at high compression (D < 150 nm), where $\phi_L \sim 0$, to a viscoelastic liquid at large separations (D > 210 nm), as $\phi_L \rightarrow 90$. This finding ties in with the observations mentioned in points ii and iii.

(v) Finally, plots for the effective mobility are shown in Figures 5 and 6, for the PHSA and PEO/PS systems, repectively. These data provide a summary of the impact of the polymer layers on the flow properties of the confined system. The term is derived from the

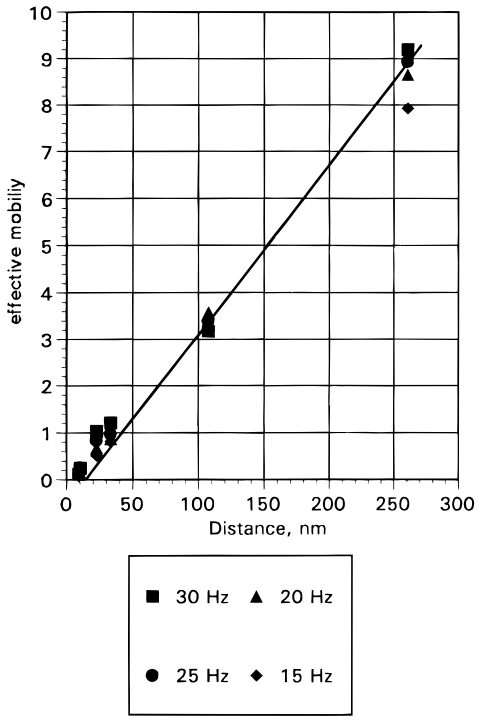

Figure 5. Plot of the effective mobility, $G \times 10^5$, as a function of separation for PHSA in decahydronaphtalene.

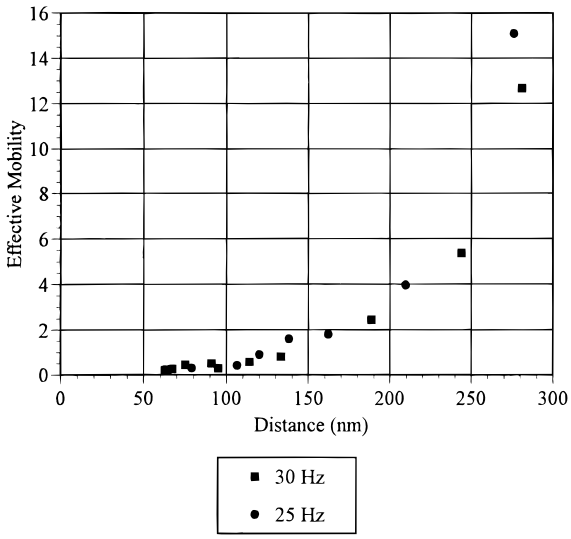

Figure 6. $G \times 10^5$, as a function of separation for PEO/PS in toluene. The arrow marks the point corresponding to the onset of interaction between the two layers, as taken from Figure 3.

equation of motion (eq 1) and is defined by

$$\frac{6\pi R^2 \omega}{k[(A_0/A)^2 - 1]^{1/2}} = G = \frac{D}{\eta} \tag{7}$$

where G is the effective mobility, and all the other symbols take on the same meaning as before. The effective mobility was introduced by Israelachvili[8] and used by a number of other workers[13,14] for three principal reasons: (a) it allows the effective position of the plane of no slip to be defined, (b) the bulk solution viscosity can be determined from the inverse of the slope of the plot away from overlap, and (c) it is a measure of the ease with which the two surfaces can be forced together or apart—the larger the value the greater the ease.

In fact, this equation only holds if the spring constant, k, is considerably larger than the force gradient, f (obtained from the force distance profile), and the gap amplitude, A, is very much smaller than the gap separation, D.

As mentioned before, it is also possible to calculate a value for the viscosity of the system from the inverse of the gradient for the plot of the effective mobility, G, — see eq 7. This suggests a value for the viscosity of ∼2.70 mPa s and compares well with the bulk viscosity of ∼2.35 mPa s. It is interesting to note however, that the plot for the effective mobility seems to support the case for a degree of flow penetration as demonstrated by the intercept on the x-axis corresponding to a distance of ∼15 nm. This value is similar to that which is predicted by the work of Milner,[31] where the plane of no slip is located at a distance corresponding to 60% of the brush thickness. Although a larger data base would be more convincing, the data do seem to lend themselves to the prediction of a significant amount of flow penetration.

For the PEO/PS system it is quite apparent that the polymer layers play a significant role in modifying the observed properties of the system. The dramatic change in the gradient away from overlap, D > 210 nm, indicates a reduced system viscosity and an increased mobility.

Discussion

In comparing the data obtained for the PHSA system, with the bulk rheological studies of other workers on colloidal particles stabilized by PMMA/PHSA in a hydrocarbon solution,[22,23] it was found that the moduli measured in the bulk studies were considerably larger than those obtained here. This is mainly as a consequence of the particles themselves contributing to the measured moduli. It is therefore difficult to make a quantitative comparison between the two forms of measurement. However, a qualitative comparison between the results is possible.

The bulk rheological studies of Strivens[23] on such systems (PHSA-stabilized PMMA latex particles) suggest that elasticity can arise from hydrodynamic effects and should not be attributed purely to colloidal forces. The observation in these experiments of a significantly larger hydrodynamic storage modulus, G_H', than a static storage modulus, G_c, (which is a function of the equilibrium forces), at all separations, supports this argument. In addition, the results for the PHSA system and the PEO/PS system also confirm the finding of Strivens[23] that the storage modulus is very much smaller than the loss modulus (i.e. $G'' \gg G'$) at volume fractions which correspond to gap separations beyond polymer layer overlap, with the situation reversed (i.e. $G' > G''$) where there are polymer interactions.

In interpreting the data obtained at large separations away from polymer interactions, it was noticeable that the values returned for the viscosity were very similar to those of the pure solvent, especially in the case of the PHSA system for D > 33 nm. This, is an interesting result as one would expect the polymer layers to behave merely as extended surfaces, with minimal participation in the flow, when the gap separation is very much greater than the layer thickness. For the PHSA system, the viscosity spans the range 2.12−2.70 mPa s, if the values obtained at 33 nm are ignored. The tables show two values for the moduli at these separations, the ones in boldface correspond to a gap separation corrected for by subtracting the polymer layer thickness, and those in italics correspond to a value obtained when the subtracted amount is equivalent to a hydrodynamic layer thickness suggested by Milner[27] (60% of the adsorbed layer thickness). From this, it is quite apparent that the calculations based on a hydrodynamic layer thickness equal to the layer thickness predict lower values for the moduli, and therefore the viscosity, than those which account for a degree of flow penetration. It is unclear at present as to which of these values is the more appropriate as the information presented in these regions is not as substantial as that presented in regions where there are strong interactions. Knowledge of the exact location of the plane (also known as the plane of no slip) beyond which the contribution of the polymer layers is minimal is a rather useful quantity as it would shed some light on the influences that determine the nature of the interactions between the layers and the solvent. For example, the work of Milner[27] suggests that the nature of the assumed adsorbed layer profile for terminally attached layers is likely to influence the extent of flow penetration. By then assuming a more realistic (near) parabolic profile[28] than the step function profile suggested by de Gennes,[29] he goes on to predict that only a region of the adsorbed layers can be considered to behave as an extended surface. The work of Klein,[13,14] however, disputes this claim as their results point to no interpenetration at low frequencies (ω < 1 Hz)—results at higher frequencies may have suggested the possible impact of frequency on the interactions between the layers and the solvent. In addition, locating the position beyond which there is minimal polymer layer participation would have enhanced the accuracy of the values quoted in the tables. This position has been located in the past by making use of the plots for effective mobility.[8,13,14] The results for this system does not allow an estimate to made for the position of the plane of no slip. However, in the particular case of the PHSA system, the values calculated, both with and without flow penetration, compare favorably with values quoted in literature of ∼2.35 mPa s at 20 °C,[30] the viscosity of the bulk solution.

The fact that the measured values do not correspond exactly to that of the bulk solution can be attributed to a number of further factors, of which that of experimental error in the measurement of amplitude and phase is probably less significant than that which is introduced as a result of the drift in the apparatus, at separations beyond overlap. The effects of this cannot be discounted as the measurement of gap separation to nanometer accuracy are hampered under these conditions. In fact it would be more realistic to suggest that the measured separations have an accuracy of ∼5% at best under these circumstances. It should be noted though, that the measurement of a slightly larger viscosity, as suggested by all the calculations corresponding to a degree of flow penetration (values in italics), than that presented in literature, would not be completely unexpected as there will be some unadsorbed polymer in the solution.

Similar conclusions could not however be drawn with the results for the PEO/PS system under similar conditions. The primary cause for this is likely to be the unacceptably large gap amplitudes. Although Israelachvili[8] has reported minimal errors, for pure solvents, when gap amplitudes were such that $A/D \sim 0.5$, polymer layers may well come into contact at such large gap amplitudes which would violate the assumption of uniform properties within the gap.

The errors found in the PEO/PS system can also be attributed to two other factors. The first of these deals with the fact that none of the readings were taken at sufficiently large separations away from overlap. At best, the readings were taken at distances of ~300 nm, which when compared to a layer thickness of 210 nm may not have been large enough for the assumption of uniform properties within the gap to be met, especially in the light of the gap amplitudes at these separations. The data obtained at such separations should perhaps be treated in terms of a three fluids analysis—a polymer layer on each of the two surfaces and the intervening fluid. The model does not provide such an analysis, and this may also explain the nature of the results obtained at 33 nm for the PHSA system. The results for the PHSA system lend weight to this argument in that it is only at a substantial distance away from overlap (values quoted at 107 and 260.1 nm) that the system exhibits bulk solvent properties—the readings obtained at 33 nm do not predict bulk viscosity, nor do they show a significantly larger loss modulus, G'', than the hydrodynamic storage modulus, G_H'. It was not possible to take readings at larger separations in the case of the PEO/PS system, as clamp changes in the Inchworm meant that it was no longer possible to locate the fringe of interest in the eyepiece, which when combined with the effects of drift made such measurements unreliable. The second factor is concerned once again with the location of the plane of no slip. For the PEO/PS system, the measurements away from overlap were made at separations far too close to the layer thickness for the impact of significant flow penetration to be ignored. If the tables for the PHSA and PEO/PS systems are compared, it is quite apparent that accounting for flow penetration in the PEO/PS system has a greater impact on the measured moduli. This is simply due to the fact that at a separation of 250 nm, e.g., the impact of flow penetration would cause a change of less than 5% in the measured moduli of the PHSA system, whereas for the PEO/PS system this would result in a 40% change, which is far from negligible.

Model Applicability. It was interesting to note that, in the case of work involving both systems, there was a certain amount of surface deformation taking place at maximum compression. This was noticeable as the fringes, though not in hard contact, did not exhibit the curvature one would expect away from contact. This suggests some deformation of the mica surfaces/glue at maximum compression. In the case of the PHSA system, the results presented below 10 nm correspond to readings taken with a "flattened" fringe, and for the PEO/PS system the slightly flattened appearance of the fringes were exhibited up to separations of ~ 55 nm. This introduces an element of error in the measurements made at such separations as flattening would have the effect of modifying the geometry of the system. A modification of the geometry would no longer allow the results to be interpreted in terms of the basic sphere on a flat model. In addition, the results also exhibit a rather curious feature in the case of the PHSA system at separations >10 nm and for the PEO/PS system at separations >100 nm. Under such circumstances, the loss modulus, G'', was seen to drop off quite markedly, and in the PHSA system this modulus was in fact seen to be smaller than that exhibited in free solution, which is a rather unrealistic result. The most likely explanation for this observed behavior must be the inapplicability of the model used to interpret data. The gap amplitude was considerably smaller than the gap separation during these readings, and the measured signals were also significantly smaller, for the effects of experimental error to be reduced. The primary reason for this must then be the nonuniform segment density profile of the polymer, at large separations, due in part to the polydispersity of the polymer, which, although small, is still significant. Such a polymer profile is incongruent with the model which relies on the medium between the two surfaces being uniform.

When the aforementioned points are taken into consideration, it is apparent that a considerable amount information relating to the behavior of the PHSA system is lost. Although there is some loss of information when measurements were carried out on the PEO/PS system, the effect on this system was rather less significant than that on the PHSA system, simply due to the fact that it was a larger polymer with a longer range of interaction. Consequently, the data obtained with the PEO/PS system are rather more reliable than those obtained with the PHSA system. Furthermore, in the particular case of this apparatus, the PEO/PS system exhibited a reduced sensitivity to the amplitude ratio. Although the amplitude ratio at maximum compression, A_o/A, was found to exceed 100 for both systems, the results point to moduli for the PEO/PS system appreciably larger than those of the PHSA system. There is no reason why this should be a real effect, as at such high compressions one would expect similar magnitudes for the moduli, at least—if anything, one would expect slightly higher values for the hydrodynamic moduli of the PHSA system, as decahydranaphthalene is a considerably more viscous substance than toluene. Consequently, the difference between the results can be attributed to the fact that the gap separation corresponding to maximum compression for the PEO/PS system is nearly an order of magnitude larger than that of the PHSA system (50 nm for the PEO/PS system compared with 6 nm for the PHSA system). Interestingly, the measured moduli for the PEO/PS system, also seem to be larger by such a factor!

Finally, the expressions for the hydrodynamic and static moduli raises a rather fundamental question with regards to the validity of a comparison between the two types of interaction (the hydrodynamic and the compressional). This can be illustrated by examining the expression for G_c (see eq 4). In this expression, the term "f/R" is apparatus independent, as it is simply the gradient of the normalized force. The basic point behind the use of a concept such as the normalized force is that it allows qualitative as well as quantitative comparison between the results of different groups—i.e., it is independent of the apparatuses used. However, in the above equation the (second) division by the radius of the surfaces, R, then results in the measured moduli being apparatus specific, even for the same systems. However, the expressions for the hydrodynamic moduli (G_H' and G''—eqs 2 and 3) may not be apparatus specific, as the complex modulus, G^*, obtained by making use of the identity

$$G^* = G' + iG'' \tag{8}$$

where

$$G' = G_H' + G_c \tag{9}$$

and, $G_c = 0$, away from overlap would not yield bulk solution viscosity ($\eta^* = G^*/\omega$) away from overlap as

reported here, and by other workers. This does therefore introduce a cautionary note with respect to conclusions drawn with respect to relaxation mechanisms. It would be unrealistic to draw wide-ranging conclusions from comparisons made between two terms, one of which is dependent on the radius of curvature of the surfaces used, and the other not.

Acknowledgment. The authors would like to thank the EPSRC and Zeneca Agrochemicals Ltd (Jealott's Hill) for the provision of a CASE studentship. Help from and discussions with Professor Th. F. Tadros, Professor S. M. Richardson, Dr. B. A. de L. Costello, Dr. C. J. Lawrence, and G. J. C. Braithwaite are also gratefully acknowledged.

References and Notes

(1) Luckham, P. F.; Costello, B. A. de L. *Adv. Colloid Interface Sci.* **1993**, *44*, 183.
(2) Fleer, G. J.; Stuart, M. A. C.; Scheutjens, J. M. H. M.; Cosgrove, T.; Vincent, B. *Polymers at Interfaces*; Chapman and Hall: London, 1993.
(3) Israelachvili, J. N.; Adams, G. E. *J. Chem. Soc. Faraday Trans. I* **1973**, *74*, 975.
(4) Luckham, P. F. *Adv. Colloid Interface Sci.* **1991**, *34*, 191.
(5) Costello, B. A. de L. Ph.D. Thesis, Imperial College, London, 1990.
(6) Van Alsten, J.; Granick, S. *Tribol. Trans.* **1989**, *32*, 246.
(7) Homola, A. M.; Israelachvili, J. N.; Gee, M. L.; McGuiggan, P. M. *J. Tribol.* **1989**, *111*, 675.
(8) Israelachvili, J. N. *J. Colloid Interface Sci.* **1986**, *110*, 263.
(9) Israelachvili, J. N.; Kott, S. J.; Fetters, L. J. *J. Polym. Sci. B.* **1989**, *27*, 489.
(10) Chan, D. Y. C.; Horn, R. G. *J. Chem. Phys.* **1985**, *83*, 5311.
(11) Horn, R. G.; Israelachvili, J. N. *Macromolecules* **1988**, *21*, 2836.
(12) Montfort, J. P.; Hadziioannou, G. *J. Chem. Phys.* **1988**, *88*, 7187.
(13) Klein, J.; Kamiyama, Y.; Yoshizawa, H.; Israelachvili, J. N.; Fredrickson, G. H.; Pincus, P.; Fetters, L. J. *Macromolecules* **1993**, *26*, 5552.
(14) Klein, J. *Colloid Surf. A* **1994**, *86*, 63.
(15) Overney, R. M.; Leta, D. P.; Pictroski, C. F.; Rafailovich, M. H.; Liu, Y.; Quinn, J.; Sokolov, J.; Eisenberg, A.; Overney, G. *Phys. Rev. Lett.* **1996**, *76*, 1272.
(16) Braithwaite, G. J. C., Luckham, P. F. L., Manimaaran, S. Submitted for publication to *Phys. Rev. Lett.*
(17) Montfort, J. P.; Tonck, A.; Loubet, J. L.; Georges, J. M. *J. Polym. Sci., B* **1991**, *29*, 677.
(18) Pelletier, E.; Montfort, J. P.; Lapique, F. *J. Rheol.* **1994**, *38*, 1151.
(19) Pelletier, E.; Montfort, J. P.; Loubet, J. L.; Tonck, A.; Georges, J. M.; *Macromolecules* **1995**, *28*, 1990.
(20) Burleigh Inchworm Instruction Manual.
(21) Stewart, A. M. *Meas. Sci. Technol.* **1995**, *6*, 114.
(22) Costello, B. A. de L.; Luckham, P. F.; Tadros, Th. F. *Langmuir* **1992**, *8*, 464.
(23) Strivens, T. A. *Colloid Polym. Sci.* **1987**, *27*, 553.
(24) Marra, J.; Hair, M. L. *Colloid Surf.* **1988**, *34*, 215.
(25) de Gennes, P. G. *Adv. Colloid Interface Sci.* **1987**, *27*, 189.
(26) Fredrickson, G. H.; Pincus, P. *Langmuir* **1991**, *7*, 786.
(27) Milner, S. T. *Macromolecules* **1991**, *24*, 3704.
(28) Milner, S. T.; Witten, T. A.; Cates, M. E. *Macromolecules* **1988**, *21*, 2610.
(29) de Gennes, P. G. *Macromolecules* **1980**, *13*, 1069.
(30) Brandrup, J.; Immergut, E. H. *Polymer Handbook*; John Wiley and Sons: New York, 1975.
(31) Milner, S. T. *Macromolecules* **1991**, *24*, 3704.

MA961186I